Interpretation of satellite structure in the x-ray photoelectron spectra of CO adsorbed on Cu(100)

R. P. Messmer
General Electric Corporate Research and Development, Schenectady, New York 12301

S. H. Lamson
3 Brookside Avenue, Albany, New York 12204

D. R. Salahub
Département de Chimie, Université de Montréal, Montréal, Québec, H3C 3V1, Canada

(Received 3 August 1981)

By employing the $X\alpha$ scattered-wave method with a Cu_9CO cluster to model the chemisorption of CO on a onefold site of a Cu(100) surface, a simple interpretation of the satellite structure observed in the x-ray photoelectron spectrum in the C 1*s* and O 1*s* regions has been obtained. The physical model obtained by analyzing the results of the Cu_9CO cluster calculations is qualitatively the same as that obtained in a previous study of a Cu_5CO cluster with the CO in a fourfold site [Solid State Commun. 36, 265 (1980)]. The qualitative differences suggest that the present Cu_9CO cluster is the better model, however. Experimentally, a three-peak structure is observed in both the O 1*s* and C 1*s* hole spectra. The "first" peak, at lowest binding energy, is followed by a second peak at 2—3 eV higher binding energy and the third peak is at 7—8 eV higher binding energy with respect to the first peak. The theoretical model derived here suggests that the unoccupied 2π level of isolated CO is split into two levels $2\tilde{\pi}_a$ and $2\tilde{\pi}_b$ on interaction with the Cu metal. In the neutral ground state neither of these levels is occupied. On the introduction of a core hole in the chemisorbed CO (e.g., the C 1*s* hole) the $2\tilde{\pi}_b$ and $2\tilde{\pi}_a$ orbitals change their character quite significantly to become $2\tilde{\pi}'_b$ and $2\tilde{\pi}'_a$. The former is now partially occupied and closely resembles the isolated 2π orbital of CO, and the latter is unoccupied with significant metal character and less CO content. The character of the 1π level of isolated CO is basically the same for the chemisorbed ground state (where it is labeled $1\tilde{\pi}$). However, it changes rather dramatically (labeled $1\tilde{\pi}'$) after the removal of the core electron, as it shifts to screen the core hole. A description of the final states which give rise to the three peaks observed in the experimental spectrum can be given in terms of the occupancies of the three orbitals $1\tilde{\pi}'$, $2\tilde{\pi}'_b$, and $2\tilde{\pi}'_a$; there is of course a 1*s* hole in each of the final states. The assignment of the final-state configuration corresponding to the three observed peaks (in order of increasing binding energy) is as follows: (1) $(1\tilde{\pi}')^4(2\tilde{\pi}'_b)^1(2\tilde{\pi}'_a)^0$, (2) $(1\tilde{\pi}')^4(2\tilde{\pi}'_b)^0(2\tilde{\pi}'_a)^1$, and (3) $(1\tilde{\pi}')^3(2\tilde{\pi}'_b)^2(2\tilde{\pi}'_a)^0$. The last final state corresponds to the final-state configuration found in the isolated CO molecule due to a $1\pi' \rightarrow 2\pi'$ shake up.

I. INTRODUCTION

The nature of the multiple lines observed in the x-ray photoelectron spectroscopy (XPS) of core levels of adsorbates on metals has received considerable attention recently. For the case of CO chemisorbed on Cu, two experimental studies have been reported.[1,2] The first studied C 1*s* and O 1*s* core-hole spectra of CO on polycrystalline Cu,[11] and the second studied the C 1*s* core-hole spectrum of CO on Cu(100).[2] Although initially the possibility of multiple adsorption sites was considered as an explanation of the observed multiple lines in the core-hole spectra, it is now generally agreed that the multiple peaks arise from a single adsorption site.[1,2]

In this paper we will discuss both the O 1*s* hole spectrum and the C 1*s* hole spectrum for CO chemisorbed on Cu(100), although it is only the latter case for which single-crystal data has been reported. However, it should be noted that the reported C 1*s* spectra for CO on polycrystalline Cu

(Ref. 1) and on Cu(100) (Ref. 2) appear very similar; both exhibit a characteristic three-peak spectrum.

The first theoretical treatment to consider the C 1*s* hole spectrum as arising from a single adsorption site for CO on Cu was the work of Gunnarsson and Schönhammer.[3] They employed a simple model Hamiltonian approach and concluded that the shape of the valence density of states (DOS) of the metal (Cu) can dramatically influence the form of the XPS core spectrum of the adsorbate. A second approach to the problem and a rather different interpretation of the origin of the three-peak spectrum was given by the present authors in a preliminary communication of results[4] associated with the present study. In that communication, as in the present work, a molecular-orbital cluster method was employed. Specifically, self-consistent-field (SCF) $X\alpha$ scattered-wave calculations[5,6] were presented for a Cu_5CO cluster in which the CO was in a fourfold site.

The third and most recent theoretical study[7] has employed a molecular cluster approach using the self-consistent-field Hartree-Fock method to study a Cu_5CO cluster, in which the CO is in a onefold site on the metal cluster. The physical model obtained from the latter study is rather different from either of the two previous studies.

Because of the rather different physical models arrived at by the three studies and the fact that a description of the physical processes is fraught with a variety of semantical difficulties, we believe it is important to review the similarities and differences found in the three works, before proceeding to describe our present results. Thus, in the remainder of the Introduction, we will present a synopsis of the salient features of the three models from a common viewpoint as well as trying to bring out the viewpoint of the individual studies. This, hopefully, will remove some of the problems which are a matter of semantics and point out the differences which are a matter of physics. We shall try always to keep in mind the actual experimental spectrum which one is trying to explain.

After this discussion, which is presented below, the computational matters related to the present work are discussed in Sec. II. The results for the various Cu_nCO clusters are given in Sec. III. In Sec. IV a discussion of the results and a comparison with experiments for transition-metal carbonyls are presented.

In Fig. 1(a) the C 1*s* XPS experimental spectrum[2] for CO chemisorbed on Cu(100) is shown.

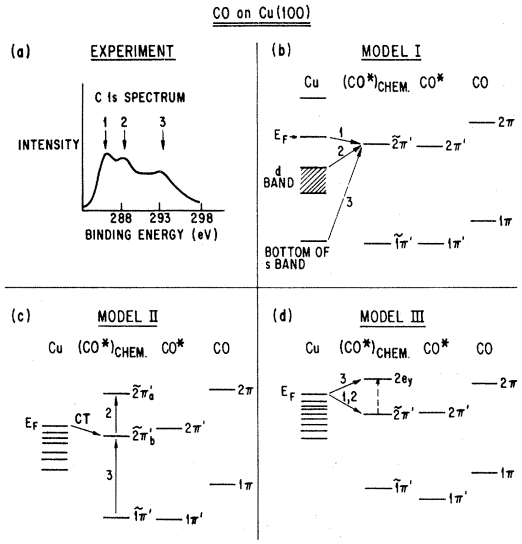

FIG. 1. Schematic representation of three interpretations of the C 1*s* photoelectron spectrum for CO chemisorbed on a Cu(100) surface. (a) represents the experimental spectrum; (b) represents the model proposed by Gunnarsson and Schönhammer (Ref. 3); (c) represents the model proposed by present authors (also see Ref. 4); (d) represents the model proposed by Bagus and Seel (Ref. 7). In (b)–(d) the rightmost column represents the 1π and 2π orbital energies of isolated CO; the column labeled CO* represents the energies of these orbitals after ionization of a C 1*s* electron. The column labeled Cu is a representation of levels near the Fermi level, and the column labeled $(CO^*)_{chem}$ shows the levels of the chemisorbed CO with a C 1*s* electron ionized. The transitions associated with the peaks in the experimental spectrum are labeled according to the interpretations of the three models. See text for discussion.

The three peaks in the spectrum are labeled to facilitate the discussion below. Naively, in a one-electron picture, one might imagine two extreme situations as a qualitative guide to the understanding of the three peaks. In the first, one can imagine that the photoionization of a C 1*s* electron from chemisorbed CO, yields three final ion states with different probabilities in which orbitals with roughly the same energies but different hole-screening capabilities are occupied in each state. These differences in hole-screening capabilities would lead to the observed differences in the C 1*s* binding energies. At the other extreme, one might imagine the situation where three different orbitals with roughly the same hole-screening capabilities are occupied in the three final states but that these orbitals have considerably different orbital energies. Thus, it would be these differences in orbital ener-

gies which would be reflected in the experimental spectrum. It should be clear however that the actual situation, expressed in one-electron terms, will most likely be a combination of these two limiting situations.

In Fig. 1(b), a schematic energy-level diagram is given which is useful in the discussion of the results of the Gunnarsson-Schönhammer (GS) model.[3] At the right of Fig. 1(b), the 1π and 2π levels of the isolated CO molecule are shown. The 1π is completely occupied with four electrons and the 2π level is empty. The occupied σ levels of CO are not shown as they are not relevant to the present discussion. At the left of Fig. 1(b) is a schematic representation of the occupied portion of the energy-level structure of Cu metal, showing the wide *sp* band overlapping the narrow 3*d* band. On introduction of a core hole in the CO molecule (labeled CO*), the 1π and 2π levels are shifted to lower energies in response to the increased positive charge on the core-hole site. Orbitals which have changed in response to a core hole are denoted with a prime. The chemisorbed CO levels are denoted by a tilde ($\sim$) over the orbital designation, and thus the $2\tilde{\pi}'$ level (which is the level of the chemisorbed molecule in the presence of the core hole) is pulled down below the Fermi level (E_F) of Cu so that a charge transfer from the metal can take place which will help to screen the core hole on CO.

The three-peak structure in Fig. 1(a) is explained by the GS model in the following manner. All three peaks are the result of the transfer of a substrate valence electron to the $2\tilde{\pi}'$ level of the CO molecule. Peak 1 results from the transfer of an *sp*-like electron which is initially close to E_F into the $2\tilde{\pi}'$ level of chemisorbed CO. Peak 2 corresponds to an *sp* electron at the top of the *d* band, $\sim$2 eV below E_F, being transferred into the $2\tilde{\pi}'$ level. Finally, peak 3 corresponds to an *sp*-like electron close to the bottom of the *sp* band "tunneling" into the $2\tilde{\pi}'$ level. The three labeled arrows in Fig. 1(b) thus schematically show the origin of the three peaks of Fig. 1(a), as determined by the GS model.

It is interesting to note that this model provides an explanation for the three-peak structure which is rather closely related to the second of the simple explanations mentioned above. That is, the screening orbital is the same in each case, and the positions of the peaks are related to the energy-level positions in the metal from which the electron is transferred, hence the conclusion of GS that the valence DOS can dramatically influence the form of the XPS core spectrum of an adsorbate.

This particular explanation of GS for CO on Cu is rather different than previous work of theirs[8] which discusses multipeak structure in core-level spectra. In previous work, a two-peak structure was discussed in terms of a screened and a nonscreened peak arising from an unoccupied adsorbate level being pulled below the Fermi level on creation of a core hole.[8] This model had been previously discussed by Kotani and Toyozawa[9] in explaining the photoelectron spectra of core electrons in La and Ce metals.

A schematic representation of the model deduced by the present authors[4] to explain the experimental spectrum of Fig. 1(a), is shown in Fig. 1(c). Again at the right are the 1π and 2π levels of the isolated CO molecule, the next column to the left shows the levels of CO with a core hole. The interaction of the 2π level of CO with Cu results in a mixing between metal and 2π producing two levels $2\tilde{\pi}_a$ and $2\tilde{\pi}_b$ (antibonding and bonding, respectively). The $2\tilde{\pi}_a$ level which is higher in energy than the $2\tilde{\pi}_b$, has far more CO 2π character than the $2\tilde{\pi}_b$ level. However, when a core hole is introduced into the chemisorbed CO producing the levels $2\tilde{\pi}'_a$ and $2\tilde{\pi}'_b$ shown in Fig. 1(c), it is found that the character of these orbitals is considerably different than those of $2\tilde{\pi}_a$ and $2\tilde{\pi}_b$. In fact, $2\tilde{\pi}'_b$ becomes more strongly CO 2π-like and $2\tilde{\pi}'_a$ becomes more strongly Cu *sp*-like. This situation will be fully discussed in Sec. III. The $2\tilde{\pi}'_b$ level, which is strongly CO 2π in character, is partially occupied with one electron. Thus, the first peak in the experimental spectrum can be attributed to a transition between the ground state of the neutral chemisorbed system and a final state in which a core hole on CO is produced together with a transfer of an electron from Cu to the $2\tilde{\pi}'_b$ orbital. This $2\tilde{\pi}'_b$ orbital containing very significant 2π CO character contributes to the screening of the core hole. It is the main contributing factor to the extramolecular screening of the core hole. This final state, i.e., the final state associated with peak 1 is the calculated ground state of the chemisorbed core-hole-ion system.[10(a)]

If one chooses this ion state as the zero of energy for discussing the spectrum of Fig. 1(a), then the other two peaks represent shakeup states as they are given by excitations from this core-hole-ion ground state. Thus, peak 2 can be viewed as a transition from this ground-state ion to an excited-state ion by virtue of an excitation of an

electron from the $2\tilde{\pi}'_b$ orbital to the $2\tilde{\pi}'_a$ orbital. Considering the character of these orbitals as discussed above, the overall transition resulting in peak 2 may be described rather well as the absence of a net charge transfer from the substrate to the chemisorbed species. Peak 3 is described as a one-electron excitation from the $1\tilde{\pi}'$ level to the $2\tilde{\pi}'$ level. This is the analog of the $1\pi' \rightarrow 2\pi'$ shakeup in isolated CO, which is found at ~ 8 eV above the main peak in the molecular core-hole spectrum (see Carlson, Ref. 10).

As a consequence of our choice of the zero of energy above, we refer to peaks 2 and 3 as "shake-up" peaks. If, however, one were to choose a zero of energy based on the isolated Cu and CO* states [first and third columns of Fig. 1(c)], one might use a different set of words to describe the spectrum although the physics remains unchanged.

Consider the consequences of basing the zero of energy on isolated Cu and CO*. The Cu cluster remains neutral; the isolated molecule is ionized, thus its $2\pi'$ level is lower than the Cu Fermi level. The final state of the interacting cluster-molecule system which most closely resembles this defined zero-of-energy state is peak 2. In this configuration the electron donated from the Cu to the $2\tilde{\pi}'_b$ has been transferred to the $2\tilde{\pi}'_a$, which also has predominantly metallic character. Then peak 1, as it is lower in energy than peak 2, must be considered a "shake-down" state. This peak is made possible by the increase screening derived from the transfer of an electron from the substrate to the molecule. Clearly the nature of the final states resulting in peaks 1 and 2 are the same regardless of how we choose the "zero-of-energy" reference point. Thus, whether we refer to peak 2 as the main peak and peak 1 as a shakedown peak, or alternatively refer to peak 1 as the main peak and peak 2 as a shake-up peak, is purely a matter of semantics—not of physics.

Bagus and Seel[7] (BS) have recently discussed a third theoretical model to explain the core-level spectrum of CO on Cu. They employed a Cu_5CO cluster and Hartree-Fock theory to discuss CO chemisorbed on a onefold Cu site. A schematic representation of the BS model is shown in Fig. 1(d). The two columns at the right are the same as for the two previous models discussed. When Cu and CO* are combined as in the second column from the left, an electron is transferred to the $2\pi'$ level of CO*, resulting in a single electron occupying the $2\tilde{\pi}'$ level of the combined system. As BS choose their reference point as the isolated Cu and CO*, they refer to this transfer of charge from the Cu to CO* as a shake-down process. They assign both peaks 1 and 2 of Fig. 1(a) to this shake-down process. They assign peak 3 as the "main peak," as the final state in this case ($2\tilde{\pi}'$ empty and one electron in $2e_y$) is almost entirely Cu in character, and hence is very similar to their reference point of isolated Cu and CO*. Note, however, that with a change in reference point one might call the first peak the main peak and the third peak a shake up [arising from the transition shown by the dotted arrow in Fig. 1(d)]. The BS model does not really explain the full three-peak spectrum of Fig. 1(a), as it does not differentiate between peaks 1 and 2. Indeed, these authors[7] only discuss the experiments in terms of a broad spectrum whose structure extends over an energy range which correlates with the energy difference between the two states considered in their calculations.

One point of agreement between the three models, in terms of the physics, is the nature of the final state which is responsible for peak 1. In all three cases this peak is said to arise from a core hole on the chemisorbed CO molecule, with an electron occupying a CO 2π-like orbital which has been transferred from the Cu sp states near the Fermi level. This is in spite of the fact that the language used to describe the situation in each of the models appears to be rather different.

However, beyond this point the agreement in terms of the basic physical situation vanishes. BS assume[7] that peak 2 has the same origin as peak 1 and the Messmer, Lamson, and Salahub (MLS) (Ref. 4) and GS (Ref. 3) models provide two further explanations. Likewise, for peak 3, the three models provide three separate explanations. Only the MLS studies have considered the possible importance of excitations involving the $1\tilde{\pi}'$ orbital. A further discussion of these models is presented in Sec. IV, following the presentation in the next two sections of the theoretical methods and the results of the present calculations.

II. THEORETICAL AND COMPUTATIONAL METHODS

A. SCF–$X\alpha$–scattered-wave calculations

The SCF-$X\alpha$-SW method has been thoroughly discussed previously and there is no need to

reiterate the basic theory. Thus, the discussion will be restricted to those aspects of the method and computations relevant to the systems under study here. A schematic representation of four Cu clusters are shown in Fig. 2. Calculations have been performed for the clusters shown in Figs. 2(a), 2(c), and 2(d). The z axis is taken as perpendicular to the page and emanating from the center of each cluster. The CO molecule is taken as collinear with the z axis, having the carbon end closer to the cluster. The "surface atoms" of each cluster are shaded in the figure. The cluster shown in Fig. 2(b) is the one chosen for the Hartree-Fock study briefly described in the Introduction. Of the Cu_5 clusters, configuration (a) represents a fourfold adsorption site and configuration (b) represents a onefold adsorption site. For the Cu_9 clusters, configuration (c) is used to represent adsorption at a onefold site and configuration (d) is used for adsorption at a fourfold site.

In our calculations the Cu-Cu distance was taken to be that of bulk Cu, i.e., $d_{nn}=2.55$ Å. Tangent Cu spheres were used in all the scattered-wave calculations, and the experimental molecular CO internuclear separation of 1.128 Å was employed. For the Cu_5CO calculations with the configuration shown in Fig. 2(a), the Cu-C distance was taken as 2.30 Å. A low-energy electron diffraction (LEED) study[11] for CO chemisorbed on Cu(100) suggests that the CO is at a onefold site with a Cu-C distance of 1.9 ± 0.1 Å. Therefore, for the Cu_9CO calculations using the configuration of Fig. 2(c), this distance was used. However, the same distance as used for the Cu_5CO model was also employed for the Cu-C internuclear separation for the configuration of Fig. 2(d).

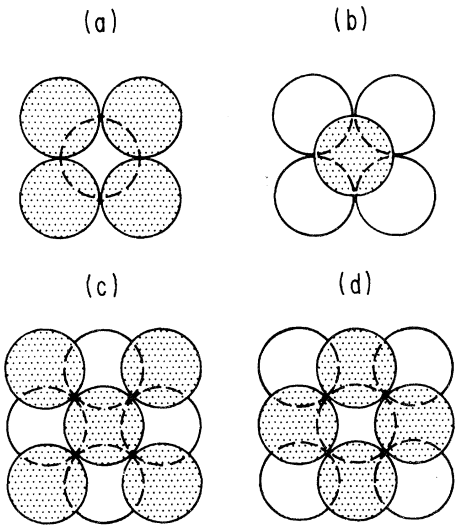

FIG. 2. Cluster geometries for Cu_5 and Cu_9 calculations. CO is positioned C-end down, perpendicular to the page at the center of each cluster. The shaded atoms denote "surface" atoms. Cluster (a) represents a fourfold adsorption site, (b) a onefold site, (c) a onefold site, and (d) a fourfold site.

The carbon and oxygen sphere radii were taken as 0.77 and 0.66 Å, respectively, constituting an overlap of 26.8% for these spheres. The atomic α values were taken from the tabulation of Schwarz[12] and the α value in the inter sphere and outer sphere regions was 0.719 80 as obtained by a weighted-atom average.[13] The partial-wave expansions included l values up to $l=1$ for carbon and oxygen spheres, $l=2$ for the Cu spheres, and $l=4$ for the outer spheres.

B. Relative intensities of core-hole states

In earlier work on core-hole states using a Cu_5CO cluster, it was found that a large number of possible final states occurred in the energy range observed for the core-hole spectrum.[14] Thus, it was necessary to calculate intensities of the various transitions in order to make a definite assignment.[4] In the latter study, as in the present one, we use a procedure first proposed by Loubriel.[15]

The intensities can be calculated assuming the sudden approximation, which is a reasonable assumption for the high energies involved in the XPS core-level ionizations. Let us assume that the initial neutral ground state (NGS) of the chemisorbed CO system is represented by a single Slater determinant:

$$\psi_i(N)=A\left[\phi_1(1)\phi_2(2)\cdots\phi_N(N)\right], \tag{1}$$

where A is the antisymmetrizer and the ϕ_i are one-electron spin orbitals. Then for simplicity we can consider two final states which are produced via the ionization of a $1s$ electron from the chemisorbed CO molecule. The final states may be written as

$$\psi_{f1}(N)=A\left[\chi_1(1)\phi_2'(2)\cdots\phi_N'(N)\right], \tag{2}$$

and

$$\psi_{f2}(N)=A\left[\chi_1(1)\phi_2''(2)\cdots\phi_{N-1}''(N-1)\phi_m''(N)\right], \tag{3}$$

where $\chi_1(1)$ represents the continuum state of the ionized electron. In Eq. (2) the primes on the orbitals denote that these orbitals are not the same as in the neutral ground state, they are the relaxed or-

bitals of the final state. We shall refer to the orbitals in Eq. (2) as the ion ground-state (IGS) orbitals. The final state of Eq. (3) differs from that of Eq. (2) in that a different electronic configuration is involved, namely orbital m is occupied rather than orbital N. The double primes in Eq. (3) denote the fact that these orbitals may be slightly different than in Eq. (2), i.e., the relaxation in the two final states may be somewhat different. We refer to the orbitals in Eq. (3) as the ion excited-state (IES) orbitals. In the sudden approximation, the ratio of the peak intensities resulting from transitions from the ground state to the two final states is

$$\frac{I_{f2\leftarrow i}}{I_{f1\leftarrow i}}=w\frac{|\langle A[\phi_2''\cdots\phi_{N-1}''\phi_m'']\,|\,A[\phi_2\cdots\phi_{N-1}\phi_N]\rangle|^2}{|\langle A[\phi_2'\cdots\phi_N']\,|\,A[\phi_2\cdots\phi_N]\rangle|^2}\,, \tag{4}$$

i.e., the ratio of the squares of overlap integrals multiplied by a factor, w, which takes account of the degeneracies of the states involved. The overlap integrals in Eq. (4) are between $(N-1)$-electron states in which the orbitals describing the ionized electron have been deleted from the N-electron states. If we represent the initial-state wave function with the $1s$ electron removed as $\psi_i(N-1)$ and represent the two final-state $(N-1)$-electron wave functions as $\psi_{f2}''(N-1)$ and $\psi_{f1}'(N-1)$, then Eq. (4) can be rewritten as

$$R=\frac{I_{f2\leftarrow i}}{I_{f1\leftarrow i}}=w\frac{|\langle\psi_{f2}''(N-1)\,|\,\psi_i(N-1)\rangle|^2}{|\langle\psi_{f1}'(N-1)\,|\,\psi_i(N-1)\rangle|^2}\,. \tag{5}$$

While the primed and double-primed wave functions are different from each other, one may expect, however, that the largest relaxation effects will occur on introduction of the core hole and that a different occupancy of valence orbitals in the final states will not produce a large change in the orbitals. That is, it is likely that the orbitals of the $\psi_{f2}''(N-1)$ and $\psi_{f1}'(N-1)$, the IGS and IES orbitals, will be quite similar. Our experience has shown that this is in fact the case. This would allow a reasonable description of $\psi_{f2}''(N-1)$ in terms of the orbitals of $\psi_{f1}'(N-1)$, i.e., $\psi_{f2}''(N-1)\simeq\psi_{f2}'(N-1)$. Thus,

$$R\simeq w\frac{|\langle\psi_{f2}'(N-1)\,|\,\psi_i(N-1)\rangle|^2}{|\langle\psi_{f1}'(N-1)\,|\,\psi_i(N-1)\rangle|^2}\,. \tag{6}$$

An additional level of approximation is possible if only a few orbitals are involved in the processes under consideration. For example, if orbital ϕ_N of the initial state becomes ϕ_N' in the state ψ_{f1}', and if an electron is excited from ϕ_N' to ϕ_m' to give state ψ_{f2}', then Eq. (6) can be approximately written as

$$R=w\frac{|\langle\phi_m'\,|\,\phi_N\rangle|^2}{|\langle\phi_N'\,|\,\phi_N\rangle|^2}\,, \tag{7}$$

which is a ratio of squares of one-electron overlap integrals.

The calculation of the one-electron overlap integrals between the initial- and final-state orbitals necessary to evaluate expressions (5)–(7) employs the method of Loubriel.[15] The radial integration is done numerically within each atomic sphere and beyond the outer sphere. The overlap integral in the intersphere region is transformed by Gauss's theorem to a surface integral over the atomic and outer spheres which bound the intersphere region. Although this technique can be derived rigorously for the touching-sphere case, its use for overlapping atomic spheres must be justified empirically. As will be discussed shortly for the case of the isolated CO molecule, the intensities calculated using overlapping spheres are reasonably close to the values obtained using touching spheres. The difference between the two sets of values is indicative of the uncertainty in the calculated intensities.

Before discussing some results for the CO molecule, it is instructive to consider a more detailed analysis[16] of the photoemission-intensity expression for the case where the initial and final states are each represented by a Slater determinant. For this situation the expression for the transition moment is

$$\begin{aligned}T_{f\leftarrow i}&=\langle\psi_f(N)\,|\sum_{k=1}^{N}\nabla_k\,|\,\psi_i(N)\rangle\\&=\langle\chi\,|\,\nabla_1\,|\,\phi_1\rangle\langle\psi_f(N-1,\chi,1)\,|\,\psi_i(N-1,\phi_1,1)\rangle+\sum_{j=2}^{N}(-1)^{1+j}\langle\chi|\,\nabla_i\,|\,\phi_j\rangle\langle\psi_f(N-1,\chi,1)\,|\,\psi_i(N-1,\phi_j,1)\rangle\\&\quad+\sum_{j=1}^{N}(-1)^{1+j}\langle\chi\,|\,\phi_j\rangle\left\langle\psi_f(N-1,\chi,1)\left|\sum_{k=2}^{N}\nabla_k\right|\psi_i(N-1,\phi_j,1)\right\rangle,\end{aligned} \tag{8}$$

where $\psi_i(N)$ is the initial-state wave function, $\psi_f(N)$ is the final-state wave function which has one electron in the continuum orbital χ, and $\psi(N-1,\phi_j,1)$ is an $(N-1)$-electron determinant constructed from the N-electron determinant by deleting the column containing orbital ϕ_j and the row containing electron 1. The intensity is proportional to the square of Eq. (8). Considering only the first term in Eq. (8) yields the sudden approximation result, which is used in Eq. (5).

If we neglect the third term in Eq. (8), the first two terms can be summarized as a single $N\times N$ determinant with the column corresponding to the continuum orbital in the final state consisting of the elements

$$\langle\chi\,|\,\nabla_1\,|\,\phi_1\rangle,\langle\chi\,|\,\nabla_1\,|\,\phi_2\rangle,\ldots,\langle\chi\,|\,\nabla_1\,|\,\phi_i\rangle\ .$$

This can most easily be visualized as using $(\nabla_1\,|\,\chi\rangle)$ as the first orbital in constructing the Slater determinant for the final state, then taking the product with the initial state.

An approximate evaluation of this $N\times N$ "augmented" determinant is to set all the matrix elements $\langle\chi\,|\,\nabla_1\,|\,\phi_i\rangle$ to a constant. This constant will factor out of the expression for the determinant. In taking the relative intensity of a shake-up peak to the principal peak, the constant will cancel. Thus, we may as well assign a value of unity to the column of the determinant due to the photoelectron in the continuum final state.

In order to discuss the intensity calculations for the CO molecule and the alternative approaches available, we wish to summarize our terminology. The determinantal wave function for the initial neutral ground state (NGS) will be constructed from the NGS orbitals. The orbitals in the ion state corresponding to the principal ionization peak are the ion ground-state (IGS) orbitals. For any shake-up peak, the orbitals of the final state will relax in response to the shake-up excitation as well, thus this final state is constructed from the ion excited-state (IES) orbitals.

The intensity of a satellite peak ought to be calculated using the overlap between two determinantal functions made up of IES orbitals and NGS orbitals, respectively. The difficulty with such a procedure is that the determinantal function constructed from the IES orbitals (to describe the shake up) is not orthogonal to the function constructed from the IGS orbitals (to describe the principal peak). Hence, the calculation of relative intensities based on overlap integrals between these states and the state constructed from neutral ground-state orbitals is not valid.

Clearly this difficulty is a consequence of the single-particle approximation and could be eliminated by going beyond the single determinantal description. This nonorthogonality can be avoided, however, by constructing the shake-up state determinant with the IGS orbitals. Although this ignores the relaxation of the orbital due to the shake up itself, it retains orthogonality of the configurations due to the orthogonality of the one-electron orbitals.

To investigate these effects, calculations on CO were considered. The calculational parameters are given in Table I. The effects of even a modest (5–7 %) configurational overlap (nonorthogonality) are shown by the results of Table II. The relative intensities (shake up to main peak) presented in Table II have been calculated using the following methods: (a) method I—augmented determinants constructed from IGS orbitals, (b) method II—augmented determinants constructed from IES orbitals, (c) method III—constructed a two-configuration excited state from the IES orbital

TABLE I. Parameters for CO molecule calculations. The CO bond distance is 2.132 bohrs.

Parameter	Region C	Region O	Region Outer sphere	Region Inter sphere
α	0.759 28	0.744 47	0.751 88	0.751 88
sphere radius[a] (tangent)	1.15	0.98	2.13	
sphere radius[a] (overlapping)	1.455	1.247	2.417	
maximum l value	1	1	2	

[a]Values are in bohrs (1 bohr=0.52918 Å).

TABLE II. Comparison of methods for calculating relative intensities of shake-up peaks. Intensities are in percent relative to the main peak.

Method		Tangent spheres				Overlapping spheres	
		I	II	III	IV	I	IV
O 1s	$1\pi\rightarrow 2\pi$	15.4	25.0	12.7	15.4	14.8	14.8
O 1s	$5\sigma\rightarrow 6\sigma$	0.3	0.9	0.3	0.3	0.5	0.6
C 1s	$1\pi\rightarrow 2\pi$	8.1	4.3	8.5	8.1	8.0	8.0
C 1s	$5\sigma\rightarrow 6\sigma$	5.6	7.5	5.2	5.7	3.3	3.3

configuration (as in method II) and the IGS configuration, such that this state is orthogonalized to the IGS configuration, and (d) method IV—using one-electron integrals, i.e., Eq. (7). A comparison of methods I and IV for overlapping spheres is also given in Table II.

Method III is closest to the ideal approach—a proper configuration-interaction (CI) calculation. We note that despite a seemingly small configuration overlap, using the IGS orbitals to construct the excited state (method I) does agree quite closely with the best estimate which we can make (method III). It is also important to note the close agreement between method I and method IV. As the latter only involves the ratio of squares of one-electron overlap integrals as in Eq. (7), this is a particularly simple and useful approximation. It is this approximate form which we will rely upon in discussing intensities in Sec. III; however, we have checked its reliability for the Cu_5CO case and found it to be very good.

III. RESULTS

A. The CO molecule

As we are concerned with the core-hole spectrum of chemisorbed CO, it is important to have an understanding of the satellites found in the core-hole spectrum of the isolated CO molecules. In this way, we can differentiate those effects which are intramolecular from those which are extramolecular in the chemisorbed spectrum. Furthermore, it is important to test our theoretical procedures on a simple system before investigating the more complicated chemisorption case.

Consider the case of $1\pi\rightarrow 2\pi$ shake up in carbon monoxide. The final-state configuration can be any of the following:

$$[(1s\alpha)^1(1\pi_x\alpha)^1(2\pi_x\alpha)^1] ,$$

$$[(1s\alpha)^1(1\pi_x\alpha)^1(2\pi_x\beta)^1] ,$$

$$[(1s\alpha)^1(1\pi_x\beta)^1(2\pi_x\alpha)^1] ,$$

or

$$[(1s\beta)^1(1\pi_x\alpha)^1(2\pi_x\alpha)^1] ,$$

where only the open-shell orbitals are shown explicitly in the configuration notation. The configuration with π_y orbitals replacing the π_x orbitals are of course degenerate, and a combination of these configurations would have to be taken to obtain a proper eigenstate of the system. The first configuration would be a spin eigenstate (a quartet). However, the other three configurations are not proper spin eigenstates— they are combinations of two doublets.

Thus, there are three unique final-energy states which can arise from a $1\pi\rightarrow 2\pi$ shake-up transition: one quartet and two doublets of which only the doublets are "allowed" transitions. The only rigorous way of calculating the two doublet excitation energies and intensities is through configuration interaction. However, the $X\alpha$ method cannot give the separate excitation energies of these doublets, and as described in the last section the procedure for calculating intensities is based on a single determinant.[17(a)] Thus, our treatment, in common with previous work on the subject,[7] is rather approximate. It is, however, sufficiently accurate to account for the main features of the experimental spectra at a semiquantitative level.

The experimental spectra are taken from two sources: the C 1s spectrum is that of Gelius[17(b)] and the O 1s spectrum is from Carlson *et al.*[10] Table III compares the experimental spectra to the values calculated using spin-restricted $X\alpha$ theory. Energies and intensities were calculated for four shake-up transitions. The total shake-up intensity calculated theoretically agrees reasonably well with the observed total, which is somewhat reassuring. However, there is clearly not a one-to-one correspondence between theory and experiment.

TABLE III. CO core-level spectrum spin-restricted calculations.

Experiment		Theory		
ΔE[a] (eV)	Intensity[b] (%)	ΔE[a] (eV)	Intensity[b] (%)	Shake-up transition
		C 1*s* region		
8.3	3.1	8.6	8.0	$1\pi\rightarrow 2\pi$
11.4	0.3			
14.9	5.6			
17.8	2.6			
19.1	2.0	19.3	3.3	$5\sigma\rightarrow 6\sigma$
20.0	1.4	22.4	3.1	$1\pi\rightarrow 3\pi$
20.8	0.6	22.9	1.2	$5\sigma\rightarrow 7\sigma$
23.2	3.9			
		O 1*s* region		
8.6	0.6			
15.6	7	13.1	14.8	$1\pi\rightarrow 2\pi$
18.0	3.7	16.1	0.6	$5\sigma\rightarrow 6\sigma$
23.8	1.5	19.7	0.5	$5\sigma\rightarrow 7\sigma$
26.5	1.2	24.6	2.5	$1\pi\rightarrow 3\pi$

[a]Shake-up energies with respect to main peak.
[b]Intensity relative to main peak.

For the spin-polarized $X\alpha$ results in Table IV, there is considerable improvement, but the fact that the excited doublet wave functions are constructed as single determinants leads to uncertainty as to the individual energies and the division of intensity between the two actual doublet final states.

Referring to Table IV, we see that for the C 1*s* spectrum the energy of the observed first peak

TABLE IV. CO core-level spectrum spin-polarized calculations (see footnotes to Table III).

Experiment		Theory		
E (eV)	Intensity (%)	E[a] (eV)	Intensity (%)	Shake-up transition
		C 1*s* region		
8.3	3.1	9.4	8.0	$1\pi\rightarrow 2\pi$
11.4	0.3			
14.9	5.6			
17.8	2.6			
19.1	2.0	19.7	3.3	$5\sigma\rightarrow 6\sigma$
20.0	1.4			
20.8	0.6			
23.2	3.9	22.1	3.1	$1\pi\rightarrow 3\pi$
		23.2	1.2	$5\sigma\rightarrow 7\sigma$
		O 1*s* region		
8.6	0.6			
15.6	7	13.5	14.8	$1\pi\rightarrow 2\pi$
		15.2	0.6	$5\sigma\rightarrow 6\sigma$
18.0	3.7	18.6	0.5	$5\sigma\rightarrow 7\sigma$
23.8	1.5	24.8	2.5	$1\pi\rightarrow 3\pi$
26.5	1.2			

[a]This is the average shake-up energy of a pair of doublets. See Ref. 17(a).

agrees reasonably well (difference of 1.1 eV) with the calculated average doublet $1\pi \rightarrow 2\pi$ transition. The intensity is overestimated, but some of this intensity will belong to the other allowed $1\pi \rightarrow 2\pi$ doublet state. Gelius[17(b)] attributes the small peak at 11.4 eV to inelastic scattering. Thus, the second calculated doublet probably corresponds to the observed peak at 14.9 eV. This assignment is consistent with a CI calculation by Guest *et al.*,[18] and with the recent discussion given by Freund and Plummer.[19] The band of shake-up peaks between 17 and 24 eV is rather well described by the calculated energies and intensities for $5\sigma \rightarrow 6\sigma$, $5\sigma \rightarrow 7\sigma$, and $1\pi \rightarrow 3\pi$ shake ups, although these assignments must be considered tentative. There can be no doubt, however, of the importance of CI in describing the shake-up states arising from $1\pi \rightarrow 2\pi$ transitions.

Although the O 1*s* experimental spectrum has fewer peaks, this may reflect the lower resolution of the spectrum. The average of the calculated $1\pi \rightarrow 3\pi$ doublets corresponds nicely to the average of the observed peaks at 23.8 and 26.5 eV. Assignment of the $1\pi \rightarrow 2\pi$ peaks is less clear. The most reasonable explanation is that there is a large correlation effect arising from the interaction of the two doublet states which will shift the first calculated $1\pi \rightarrow 2\pi$ doublet to align it with the observed 8.6-eV peak and allow the second $1\pi \rightarrow 2\pi$ doublet state to explain the 15.6-eV peak. There is considerable support for this interpretation in the consistent appearance of a 7–8-eV shake up in transition-metal carbonyls and in CO chemisorbed on transition-metal surfaces.[19] An O 1*s* $1\pi \rightarrow 2\pi$ shake up around 8 eV would thus explain the observation of this peak in such a variety of environments.

Only through a careful CI calculation will the assignment of the shake-up spectrum of CO be fully resolved. However, higher-resolution experimental data also will be required in order to determine the accuracy of such calculations.

B. Cu_9CO calculations

The calculations for Cu_9CO with CO at the one-fold site [cf. Fig. 2(c)] at a Cu–C distance of 1.9 Å (the distance determined by LEED) will be discussed first. Shown in Fig. 3(a) are the ground-state orbital energies for this cluster. The orbital energies are measured with respect to the highest occupied orbital (E_F) as the zero. This highest occupied orbital and one below it are Cu *sp*-like in

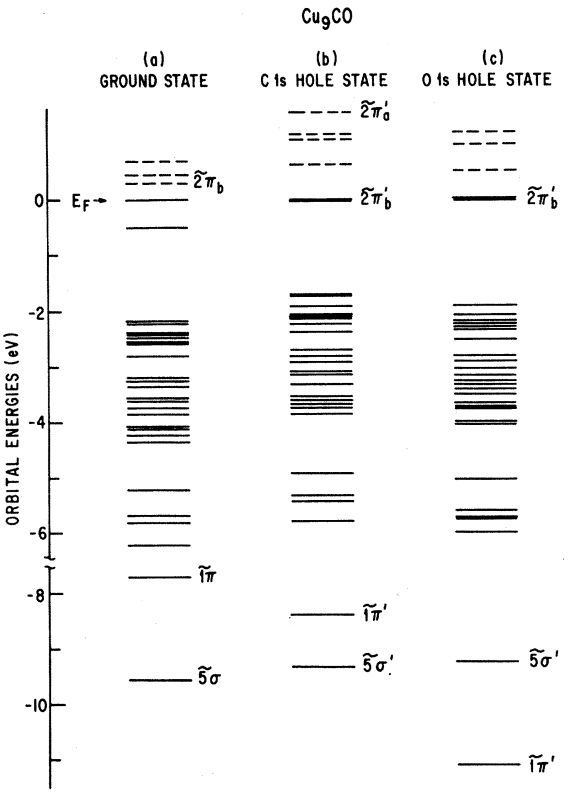

FIG. 3. Orbital energy-level diagrams determined from $X\alpha$–scattered-wave calculations for a Cu_9CO cluster. CO is positioned above the central atom of the Cu cluster shown in Fig. 2(c). The energy levels of each of the three cases have been rigidly shifted so as to align the highest occupied levels with $E_F=0$. Dashed lines represent unoccupied levels. (a) shows the ground-state orbital energies of Cu_9CO, (b) shows the orbital energies of the C 1*s* hole state, and (c) shows the orbital energies of the O 1*s* hole state. The $2\tilde{\pi}'_b$ levels in (b) and (c) contain one electron.

character. The unoccupied levels are denoted by dashed lines. The first unoccupied level is the $2\tilde{\pi}_b$ which is a mixture of Cu *sp* and CO 2π components; a contour plot of it is shown in Fig. 4. About 2 eV below E_F there is a group of closely spaced levels which are strongly Cu 3*d*-like in character with some admixture of Cu *sp* character. Below this group of closely spaced levels which constitute the cluster analog of the Cu *d* band, there are several levels between -5 to -6.5 eV which are Cu *sp*-like. Finally, starting at ~ -8 eV are the levels associated with the CO molecule. A contour plot of the $1\tilde{\pi}$ orbital is also shown in Fig. 4. The splitting between the $1\tilde{\pi}$ and $5\tilde{\sigma}$ orbitals of the chemisorbed system tends to be quite exaggerated by the muffin-tin approximation to the po-

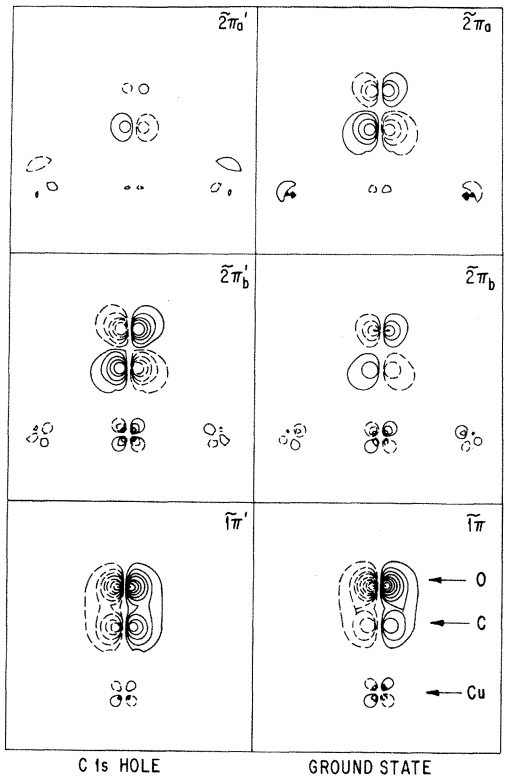

FIG. 4. Contour plots of the $1\tilde{\pi}$, $2\tilde{\pi}_b$, and $2\tilde{\pi}_a$ orbitals of chemisorbed CO on the onefold site of the Cu_9 cluster shown in Fig. 2(c). The orbitals at the right are for the ground state of the cluster before C 1*s* ionization; the orbitals at the left are for the C 1*s* hole state which results after a C 1*s* electron is ionized. The positions of the C, O, and Cu nuclei are shown in the lower-right panel. They are in the same relative orientation in the other panels. The Cu atoms show very few contours because the Cu character is mostly diffuse *s* and *p*.

tential. However, for the isolated CO molecule, this is not the case.[20(a)] Another orbital of interest is the $2\tilde{\pi}_a$ orbital [a contour plot is given in Fig. 4(a)] which is unoccupied and is not shown on the orbital energy level of Fig. 3(a) because it is too high in energy.

On the introduction of a C 1*s* core hole in the chemisorbed CO molecule, the originally unoccupied $2\tilde{\pi}_b$ is pulled down in energy such that it becomes partially occupied ($2\tilde{\pi}_b'$). Note that the $1\tilde{\pi}$ orbital is also stabilized. These CO levels are pulled down in energy relative to the Cu levels as a result of the localized core hole produced on the CO molecule. It is the orbitals of chemisorbed CO which exhibit the most dramatic response to the creation of a core hole. This is shown clearly in Fig. 4, where contour plots of the $1\tilde{\pi}$, $2\tilde{\pi}_b$, and $2\tilde{\pi}_a$ orbitals, before and after the introduction of the core hole, are given. The response of the $1\tilde{\pi}$ orbital when a C 1*s* electron is ionized, is to shift toward the carbon atom in order to screen the core hole. The response of the $2\tilde{\pi}_b$ orbital is quite dramatic. In the ground state it is unoccupied and has some CO content, but is mainly Cu in character. In the C 1*s* hole state it is occupied and is now very largely CO 2π in character. As the $2\tilde{\pi}_a'$ orbital must remain orthogonal to the $2\tilde{\pi}_b'$ orbital, there is also a significant change in the $2\tilde{\pi}_a$ orbital on going from the ground state to the C 1*s* hole state. In fact in the hole state, this orbital ($2\tilde{\pi}_a'$) is now almost exclusively Cu *sp*-like in character.

Qualitatively, a very similar situation occurs for the case of the O 1*s* hole state, with the exception of course that the $1\tilde{\pi}$ orbital shifts to the oxygen end in the O 1*s* hole state in order to screen the core hole. However, the qualitative changes in the $2\tilde{\pi}_b$ and $2\tilde{\pi}_a$ orbitals are similar to those discussed for the C 1*s* case.

In Fig. 3, Fermi statistics are obtained in each case. For the ground state, the Fermi level is determined by a metal-like $7b_2$ level which contains one electron. For the O 1*s* hole state, the $2\tilde{\pi}_b'$ level contains one electron and determines E_F. However, for the C 1*s* hole state, Fermi statistics are only satisfied if the $2\tilde{\pi}_b'$ contains a small fraction of an electron beyond an integer occupancy. The differences in wave functions, energies, etc., are rather slight between the cases of integer occupancy of $2\tilde{\pi}_b'$ and the noninteger occupancy of this orbital. As a consequence of this and the ease of dealing with integral-occupancy configurations, only those calculations which assume integer-occupation numbers will be discussed here.

Thus, the ground state of the core-hole ion has the configuration I: $(1\tilde{\pi}')^4(2\tilde{\pi}_b')^1(2\tilde{\pi}_a')^0$, and the various "shake-up" states (since we are choosing this state as our zero of energy to discuss other final states) will be obtained by electronic excitations from this configuration. As mentioned in the Introduction and as discussed below, the only transitions which have any appreciable intensity are those involving these three orbitals, the $1\tilde{\pi}'$, $2\tilde{\pi}_b'$, and $2\tilde{\pi}_a'$. The lowest excited ion state has the configuration II: $(1\tilde{\pi}')^4(2\tilde{\pi}_b')^0(2\tilde{\pi}_a')^1$, and the other excited ion state has the configuration III: $(1\tilde{\pi}')^3(2\tilde{\pi}_b')^2(2\tilde{\pi}_a')^0$. These are the three final states which give rise to the spectrum of Fig. 1(a).

In order to determine the energy separations between these three states, spin-polarized transition-state calculations were carried out. Taking config-

uration I as the zero of energy, we obtain for the C 1*s* core-hole case energy separations of 2.3 and 8.1 eV for configurations II and III, respectively. Likewise for the O 1*s* core hole, we obtain energy separations of 1.9 and 12.5 eV. For the case of configuration III, there are three open shells (including the core shell) which lead to many possible states as a result of the various allowed spin couplings. Within the context of $X\alpha$ theory the various states cannot be resolved, as one does not generate proper eigenstates of the total spin. As a consequence, the numbers quoted above are based on the high-spin configuration. Although within the context of *ab initio* calculations such spin couplings can be rigorously treated, the work of BS (Ref. 7) on Cu_5CO has not considered this problem.

In Table V the results for the shake-up intensities are presented; only those shake-up transitions are given which have calculated relative intensities greater than one percent. Again we note that the energies and intensities are given relative to the calculated first peak, i.e., the core-hole ion ground state. Only two transitions have significant intensities (these are underlined in Table V). They are the ones previously referred to as giving rise to the two satellite peaks in the spectrum of Fig. 1(a). Although the calculated relative intensities for the two satellites are not quantitative, they do have the correct behavior of decreasing in intensity with increasing binding energy, which contrasts with the behavior found in the recent Hartree-Fock cluster calculations.[7] We note that the $1\tilde{\pi}' \rightarrow 2\tilde{\pi}'_b$ peak position for the O 1*s* hole is considerably higher in energy than the corresponding peak for the C 1*s* hole. This is completely analogous to the situation seen above for the isolated CO molecule.

In Table V, the energies have been determined by the transition-state procedure for the intense transitions. For the weak transitions the energies have been estimated from the ion- and ground-state orbital energies; these values are given in parentheses.

For the case of the C 1*s* hole spectrum a further calculation was performed. In this calculation the CO-Cu distance was increased from 1.9 to 2.4 Å. Then ΔE and the relative intensity of the $2\tilde{\pi}'_b \rightarrow 2\tilde{\pi}'_a$ transition were calculated. The results for this larger distance were found to be 2.55 eV and 127% as compared to the values (at 1.9 Å) of 2.26 and 80.4% in Table V. Thus, as the Cu-CO distance is increased the intensity of peak 2 becomes larger than that of peak 1. The significance of this result will be discussed in Sec. IV.

Results have also been obtained for CO chemisorbed in a fourfold site using a Cu_9 cluster [cf. Fig. 2(d)], with the Cu-C distance of 1.43 Å as employed in the previous Cu_5CO study.[4] It is probably useful only to discuss these results in a qualitative way, pointing out the differences among the Cu_9CO (onefold site), the Cu_9CO (fourfold site), and the previous study of Cu_5CO.

The most important point, however, is that the results of all three calculations are qualitatively very similar. The same basic picture of the physics involved in producing the satellite structure obtains. The differences of interest are the following. Comparing the fourfold-site cases of Cu_5CO and Cu_9CO (4), one finds in the former case[4] that both the $1\tilde{\pi}' \rightarrow 2\tilde{\pi}'_b$ and $1\tilde{\pi}' \rightarrow 2\tilde{\pi}'_a$ transitions have roughly comparable intensities. However, in the latter case the $1\tilde{\pi}' \rightarrow 2\tilde{\pi}'_b$ transition has a calculated intensity about an order of magnitude greater than for the $1\tilde{\pi}' \rightarrow 2\tilde{\pi}'_a$ transition. Thus, the fourfold-site Cu_9CO result is similar to the onefold-site results for Cu_9CO (1) shown in Table V. A second difference between the Cu_9CO (1), Cu_9CO (4) results, and the Cu_5CO results is that in both the former cases the $2\tilde{\pi}_b$ orbital is unoccupied before the core hole is introduced. In all cases the $2\tilde{\pi}_b$

TABLE V. Results for Cu_9CO onefold-site core-level spectra. Energies and intensities are given relative to the core-hole ion ground state.

	O 1*s* core hole		C 1*s* core hole	
Transition	ΔE (eV)	Intensity (%)	ΔE (eV)	Intensity (%)
$12a'_1 \rightarrow 13a'_1$			(1.36)	1.5
$8e' \rightarrow 2\tilde{\pi}'_b$	(2.53)	2.2	(2.03)	1.6
$2\tilde{\pi}'_b \rightarrow 2\tilde{\pi}'_a$	1.86	<u>22.9</u>	2.26	<u>80.4</u>
$1\tilde{\pi}' \rightarrow 2\tilde{\pi}'_b$	12.5	<u>11.9</u>	8.09	<u>9.1</u>
$1\tilde{\pi}' \rightarrow 2\tilde{\pi}'_a$	(12.8)	1.7	(9.96)	1.1

orbital on becoming the $2\tilde{\pi}'_b$ orbital (on introduction of the core hole) loses considerable Cu character and gains CO 2π character. This effect is more dramatic for the Cu_9CO cases.[20(b)]

In Sec. II we discussed various methods for calculating satellite intensities for the CO molecule. As a consequence of the results presented there, we have restricted our subsequent discussion to results employing method IV based on ratios of the squares of one-electron overlap integrals. It is useful, however, to check the calculated intensities using this approach with that of a more rigorous approach (method I) for the case of chemisorbed CO. To this end we present in Table VI a comparison of calculated intensities for the Cu_5CO cluster. It can be seen that there is reasonable agreement between the two methods considering the approximations involved. The two entries for the $1\tilde{\pi}' \rightarrow 2\tilde{\pi}'_a$ shake up using method I arise from the fact that the N-electron wave functions used to calculate the intensities are not proper spin eigenstates. Thus, although one can derive two formally equivalent expressions for the overlap integral involved in method I, they yield two different intensities as a consequence of this defect in the present procedures. Nonetheless, these differences are not large enough to obscure the basic physics involved, and we conclude that method IV is adequate to provide a reliable approximation for the purposes of the present study. A truly quantitative evaluation of intensities would involve enormous labor, which in our view is neither justified nor feasible at present.

All of the results presented thus far have been concerned with the satellite structure found in the core-level spectroscopy of CO chemisorbed on Cu. However, there is also experimental information for the valence region of CO chemisorbed on Cu using ultraviolet photoelectron spectroscopy.[1,21] The experimental data is shown in Fig. 5. Norton *et al.*[1] suggest that the structure in the valence region of the chemisorbed CO should be considered to consist of four peaks which we have labeled with Roman numerals in the figure. However, Allyn *et al.*[21] consider peaks I and II as one peak with two components. The latter study used angle-resolved photoelectron spectroscopy (ARPES) to investigate CO on Cu(100). They showed that peak III of Fig. 5 was due to the ionization of the $4\tilde{\sigma}$ orbital of CO and that the structure in the region of I and II was due, at least in part, to the $1\tilde{\pi}$ and $5\tilde{\sigma}$ ionizations of the chemisorbed CO molecule. They assigned peak IV to a shake up (the nature of which was not specified) associated with the $4\tilde{\sigma}$ ionization.

From transition-state calculations for the Cu_9CO cluster we have calculated the ionization energies of the chemisorbed CO $1\tilde{\pi}$, $5\tilde{\sigma}$, and $4\tilde{\sigma}$ orbitals. By a rigid shift of the calculated values so as to match the $4\tilde{\sigma}$ ionization energy with the position of peak III, one arrives at the positions and assignments shown at the top of Fig. 5. It should be noted that although the calculated $5\tilde{\sigma}$ binding energy is found to fall in the proper region, the $1\tilde{\pi}$ is found at a binding energy which is too low. We have discovered from our many calculations on these systems that the $1\tilde{\pi}$ orbital energy and ionization energy is particularly sensitive to errors which arise from the muffin-tin nature of the potential used in these scattered-wave calculations. The $1\tilde{\pi}$ binding energy would undoubtedly be much closer to that of the $5\tilde{\sigma}$ if the muffin-tin errors did not occur.

The only shake-up transition calculated to have

TABLE VI. Comparison of methods for calculating relative intensities of Cu_5CO.

Transition	Methods I	Methods IV[a]
O 1s $2\tilde{\pi}'_b \rightarrow 2\tilde{\pi}'_a$	22.0	28.9
O 1s $1\tilde{\pi}' \rightarrow 2\tilde{\pi}'_b$	12.4	8.7
O 1s $1\tilde{\pi}' \rightarrow 2\tilde{\pi}'_a$	7.1 13.1	5.4
C 1s $2\tilde{\pi}'_b \rightarrow 2\tilde{\pi}'_a$	43.9	46.5
C 1s $1\tilde{\pi}' \rightarrow 2\tilde{\pi}'_b$	5.6	5.4
C 1s $1\tilde{\pi}' \rightarrow 2\tilde{\pi}'_a$	7.0 12.6	6.6

[a]Results of Ref. 4.

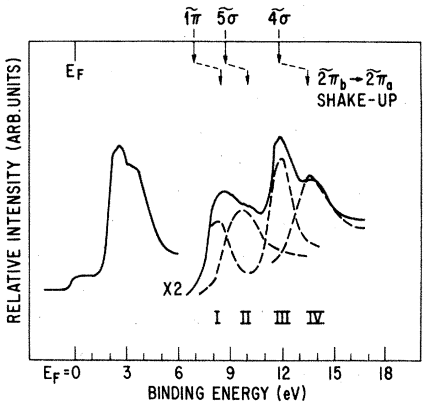

FIG. 5. Comparison of experimental ultraviolet photoelectron transition energy (Ref. 1) with calculated spectrum based on $X\alpha$—scattered-wave calculations for Cu_9CO. The calculated values were rigidly shifted so as to align the calculated $4\tilde{\sigma}$ ionization energy with peak III of the spectrum. See text for discussion.

any appreciable intensity is the $2\tilde{\pi}_b \rightarrow 2\tilde{\pi}_a$, which was also important in understanding the core region.[22] The calculated shake-up energy positions (relative to their parent orbital binding energies) are shown by the lower set of arrows in Fig. 5. Taking into account the likelihood that the $1\tilde{\pi}$ position should be closer to the $5\tilde{\sigma}$ position, we arrive at the following assignment of the structure in the spectrum. Peaks I and II arise from the primary ionizations from the $1\tilde{\pi}$ and $5\tilde{\sigma}$ orbitals together with a $2\tilde{\pi}_b \rightarrow 2\tilde{\pi}_a$ shake up which accompanies these primary ionizations. Peak III is due to the ionization from the $4\tilde{\sigma}$ orbital and peak IV is due to the $2\tilde{\pi}_b \rightarrow 2\tilde{\pi}_a$ shake up which accompanies the ionization from the $4\tilde{\sigma}$ orbital. Thus, one may understand the satellite structure in the valence as well as core regions from a simple unified point of view.

IV. DISCUSSION

In order to assess the validity and generality of the interpretation which emerges from the calculations presented in Sec. III, it is worthwhile to consider the core-level satellites of CO in a more general context; that is, to make a comparison of core-level spectra for isolated CO, molecular carbonyls, and chemisorbed CO. Such a comparison has been given by Freund and Plummer[19] and Fig. 6 is adapted from their work. We consider the O 1*s* core region of CO in different environments—free, molecular, and chemisorbed. For the

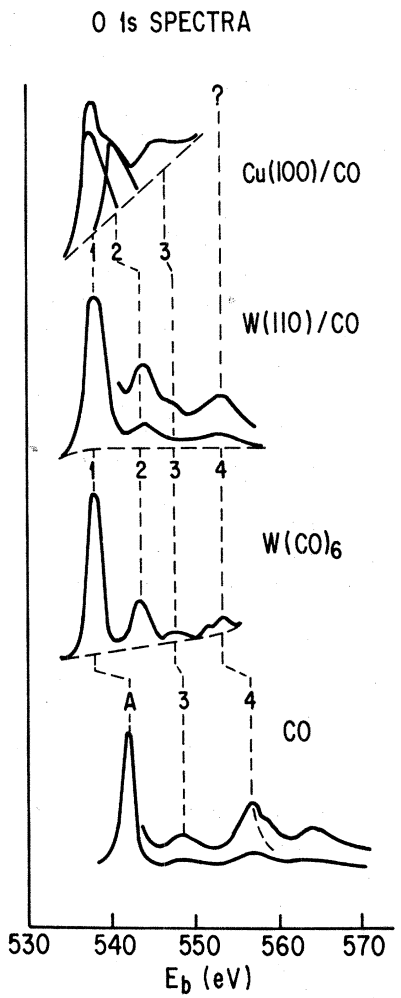

FIG. 6. Comparison of experimental O 1*s* spectra for an isolated CO molecule, the $W(CO)_6$ molecule, CO chemisorbed on W(110), and CO chemisorbed on Cu(100). Adapted from data given in Ref. 19.

free-molecule spectrum at the bottom of Fig. 6, the three peaks of interest are labeled *A*, 3, and 4. Peak *A* arises from the ionization of the O 1*s* electron, peaks 3 and 4 are shake ups which accompany the O 1*s* ionization and arise from the transition $1\pi \rightarrow 2\pi$. There are two peaks from this transition because two independent doublet states are created.

When the CO molecule interacts with a metal atom as in the case of the $W(CO)_6$ molecule, the 2π orbital of CO interacts with the metal atom so as to produce two new orbitals—a bonding $2\tilde{\pi}_b$ and an antibonding $2\tilde{\pi}_a$ orbital. The stronger the interaction between the metal and CO, the larger the energy separation between the $2\tilde{\pi}_b$ and $2\tilde{\pi}_a$ levels. Upon ionizing the O 1*s* electron, the $2\tilde{\pi}_b$ orbi-

tals should become partially occupied and pick up considerable CO 2π character (see Fig. 4 for the Cu_9CO case), this contributes screening to the core hole and results in peak 1 being at a lower binding energy as compared to peak A of isolated CO. It is also seen from Fig. 6 that a new peak arises, peak 2, which is related to peak A of the free CO molecule (see below). This peak can exist in the interacting case because the core-hole ion ground state has the $2\tilde{\pi}'_b$ orbital partially occupied (the $2\pi'$ orbital is empty in the CO case) and further, due to the energy splitting produced between the $2\tilde{\pi}'_b$ and $2\tilde{\pi}'_a$ orbitals, a transition (shake up) can occur between the $2\tilde{\pi}'_b$ and $2\tilde{\pi}'_a$ orbitals. The shake-up transition is of the nature of a ligand-to-metal charge transfer (see Fig. 4 for Cu_9CO case). Peaks 3 and 4 are shifted to lower binding energies due to the screening effects of the partial occupancy of the $2\tilde{\pi}'_b$ orbital. They arise from $1\tilde{\pi}' \rightarrow 2\tilde{\pi}'$ shake ups which are direct analogs of the molecular shake-up transitions.

For the case of CO on W(110), the explanation should be virtually identical to that of $W(CO)_6$ and one finds that the observed spectra are very similar.

Considering the situation for Cu(100)-CO, we observe that the peaks 1 and 2 are less separated than for the two previous cases. This undoubtedly arises from the fact that the Cu-CO interaction, is considerably weaker than the W-CO interaction, leading to a smaller splitting between the $2\tilde{\pi}_b$ and $2\tilde{\pi}_a$ orbitals. Thus, the shake-up transition $2\tilde{\pi}'_b \rightarrow 2\tilde{\pi}'_a$ has a lower energy. Peak 3 arises from a $1\tilde{\pi}' \rightarrow 2\tilde{\pi}'_b$ shake up. An interesting question arises in this case: If the spectrum had been recorded to higher binding energies would there be a peak 4? Clearly the systematics observed here indicate that this should be the case if the intensity is not significantly reduced from the molecular situation.

A comment with regard to the assignment of Bagus and Seel[7] is in order at this point. They maintain that peaks 1 and 2 of the Cu(100)-CO spectrum are due to shake down and that peak 3 corresponds to peak A of free CO. We know of no reason why peak A of free CO should shift to *higher* binding energies when interacting with a metal. All experience has been that the shift should be to lower binding energies due to screening effects. Bagus and Seel provide no explanation for this rather curious situation, which is a consequence of their assignments.

Another interesting way to gain some insight into the relationship between the isolated CO spectrum and that for the chemisorbed case is through Fig. 7 which has been adapted from Ref. 19. Figure 7 shows a schematic representation of the changes in the spectrum as a function of the Cu-CO distance. Curve e represents the essential features of the isolated CO molecule (cf. Fig. 6). Basically, peaks 3 and 4, which arise from $1\tilde{\pi} \rightarrow 2\tilde{\pi}_b$ shake ups, should be in roughly the same positions relative to peak 1 for all distances. For the case of CO on Cu, peak 4 has not yet been observed and hence it is designated in curves $a-d$ as a dashed-line portion of the curves.

When the isolated CO molecule interacts with the metal, peak A is split into two peaks—peaks 1 and 2 of curves $a-d$. The splitting arises from the Cu-CO 2π interaction producing the bonding $2\tilde{\pi}'_b$ and antibonding $2\tilde{\pi}'_a$ orbitals with the $2\tilde{\pi}'_b$ orbital being occupied in the case of peak 1 and the $2\tilde{\pi}'_a$ orbital being occupied in the case of peak 2. As the $2\tilde{\pi}'_b$ orbital is largely CO 2π in character and the $2\tilde{\pi}'_a$ orbital largely metal (see Fig. 4), one may view peaks 1 and 2 in curves $a-d$ roughly as the screened and unscreened counterparts, respectively, of peak A in curve e.

The binding energy separation between peaks 1 and 2 reflects the separation between the $2\tilde{\pi}_b$ and $2\tilde{\pi}_a$ levels. The stronger the interaction between the metal and CO (i.e., the shorter the bond length curve a), the larger the separation. Conversely, the weaker the interaction and longer the bond length, the smaller the separation (curve d). The trend in

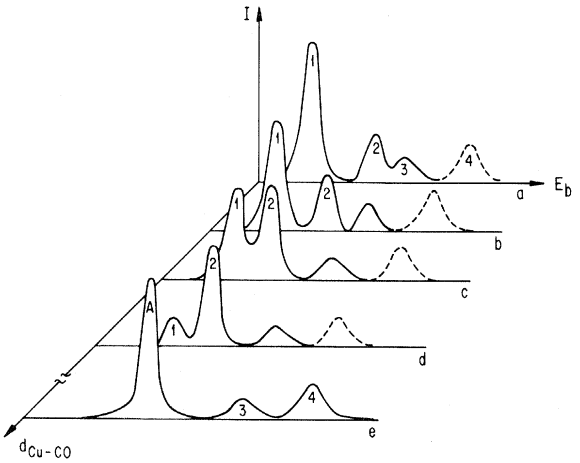

FIG. 7. Schematic representation of expected behavior of core-hole spectra as a function of Cu-CO distance. Curves $a-d$ are for increasing metal-CO distances, curve e for the isolated CO molecule.

intensities of peaks 1 and 2 may also be understood in simple terms. At large distances (curve *d*) the overlap of metal orbitals with the CO $2\tilde{\pi}'$ orbital is not very significant, thus the probability that an electron will be transferred from the metal to CO is small and the intensity of peak 1 is consequently small. However, at short distances (curve *a*) the overlap is quite significant and thus the probability that an electron is transferred is significantly increased, resulting in a larger intensity of peak 1.

It is interesting to note that for the Cu_9CO calculations with the Cu-CO distance at 1.9 Å, the results presented in the preceding section suggest a qualitative situation somewhat intermediate between curves *b* and *c*. The results for the C 1*s* spectrum at a Cu-CO distance of 2.4 Å suggest a qualitative situation intermediate between curves *c* and *d*. Thus, the calculated results clearly conform to the schematic picture represented in Fig. 7.

We believe that this model and interpretation of experimental results which emerges from the present work and our previous work has the advantage over other models of providing a coherent framework with which to view the core-hole spectrum of CO in various environments. Its viewpoint is very similar in spirit to that also espoused by Freund and Plummer[19] and consistent with the experimental information which they have discussed. Furthermore, we believe it will provide a conceptual framework with which to discuss the features of core-level spectra in other systems.

ACKNOWLEDGMENTS

One of us (R.P.M.) is grateful to E. W. Plummer and H. J. Freund for several useful discussions. This work was supported in part by the Office of Naval Research. Another author (D.R.S.) is grateful for support from National Science and Engineering Research Council (Canada) and General Electric.

[1]P. R. Norton, R. L. Tapping, and J. W. Goodale, Surf. Sci. 72, 33 (1977).

[2]J. C. Fuggle, E. Umbach, D. Menzel, K. Wandelt, and C. R. Brundle, Solid State Commun. 27, 65 (1978).

[3]O. Gunnarsson and K. Schönhammer, Phys. Rev. Lett. 41, 1603 (1978).

[4]R. P. Messmer, S. H. Lamson, and D. R. Salahub, Solid State Commun. 36, 265 (1980).

[5]J. C. Slater and K. H. Johnson, Phys. Rev. B 5, 844 (1972).

[6]K. H. Johnson and F. C. Smith, Jr., Phys. Rev. B 5, 831 (1972).

[7]P. S. Bagus and M. Seel, Phys. Rev. B 23, 2065 (1981).

[8]K. Schönhammer and O. Gunnarsson, Solid State Commun. 23, 691 (1977).

[9]A. Kotani and Y. Toyozawa, J. Phys. Soc. Jpn. 37, 912 (1974).

[10](a) Referring to Fig. 1, it should be noted that peak 1 of the spectrum [Fig. 1(a)] corresponds to the charge transfer (CT) shown schematically in Fig. 1(c). Peak 2 corresponds to CT followed by shake-up transition labeled 2 [in Fig. 1(c)] and peak 3 corresponds to charge transfer (CT) followed by shake-up transition labeled 3 [in Fig. 1(c)]. (b) T. A. Carlson, M. O. Krause, and W. E. Moddeman, J. Phys. (Paris) 32, C4-76 (1971).

[11]S. Andersson and J. B. Pendry, Phys. Rev. Lett. 43, 363 (1979).

[12]K. Schwarz, Phys. Rev. B 5, 2466 (1972).

[13]H. L. Yu, J. Chem. Phys. 69, 1755 (1978).

[14]R. P. Messmer and S. H. Lamson, Chem. Phys. Lett. 65, 465 (1979).

[15]G. Loubriel, Phys. Rev. B 20, 5339 (1979).

[16]R. L. Martin and D. A. Shirley, in *Electron Spectroscopy: Theory, Techniques, and Applications*, edited by C. R. Brundle and A. D. Baker (Academic, New York, 1977), Vol. I, p. 75.

[17](a) There are three unpaired spins in the final state, resulting in $2^3=8$ spin determinants. Two determinants are pure quartet states, $D_1=|\alpha\alpha\alpha\rangle$ and $D_2=|\beta\beta\beta\rangle$, the remaining six are doublet-quartet mixtures. The following sum rule holds: $\sum_{i=1}^{8}E(D_i)=4E_{\text{quartet}}+2E_{\text{doublet}}+2E'_{\text{doublet}}$. The E_{quartet} is known to be $E(D_1)=E(D_2)$. Although the individual energies of the doublets can be found only by solving a 2×2 configuration-interaction-like calculation, the mean energy of the pair of doublets is given by $E_{\text{av}}=\frac{1}{2}(E_{\text{doublet}}+E'_{\text{doublet}})=\frac{1}{4}[\sum_{i=3}^{8}E(D_i)-E(D_1)-E(D_2)]$. The intensity for each pair of doublets is taken from the spin-restricted method. (b) U. Gelius, J. Electron Spectrosc. Relat. Phenom. 5, 985 (1974).

[18]M. F. Guest, W. R. Rodwell, T. Darko, I. H. Hillier, and J. Kendrick, J. Chem. Phys. 66, 5447 (1977).

[19]H. -J. Freund and E. W. Plummer, Phys. Rev. B 23, 4859 (1981).

[20](a) D. R. Salahub, R. P. Messmer, and K. H. Johnson, Mol. Phys. 31, 529 (1976). (b) The total charge on CO from the $2\tilde{\pi}'_b$ orbital is about the same in both the Cu_5CO and Cu_9CO calculations. However, in the former case this orbital is occupied by three electrons, whereas in the latter case it contains only one electron. Hence, the change in the orbital on going from

$2\tilde{\pi}_b$ to $2\tilde{\pi}'_b$ is less dramatic for Cu_5CO than for Cu_9CO. See Ref. 4.

[21]C. L. Allyn, T. Gustafsson, and E. W. Plummer, Solid State Commun. 24, 531 (1977).

[22]The calculated intensities of the $2\tilde{\pi}_b \rightarrow 2\tilde{\pi}_a$ shake ups relative to the primary ionization are 13.9%, 10.6%, and 7.4% for the $4\tilde{\sigma}$, $1\tilde{\pi}$, and $5\tilde{\sigma}$ primary ionizations, respectively. The next largest intensities are for the $1e \rightarrow 14e$ and $13e \rightarrow 14e$ shake ups from the $4\tilde{\sigma}$ primary ionization which are 1.4% and 1.3%, respectively.